RESEARCH ARTICLE

A large-scale transgenic RNAi screen identifies transcription factors that modulate myofiber size in *Drosophila*

Flavia A. Graca[1], **Natalie Sheffield**[1], **Melissa Puppa**[1¤], **David Finkelstein**[2], **Liam C. Hunt**[1], **Fabio Demontis**[1]*

1 Department of Developmental Neurobiology, St. Jude Children's Research Hospital, Memphis, Tennessee, United States of America, **2** Department of Computational Biology, St. Jude Children's Research Hospital, Memphis, Tennessee, United States of America

¤ Current address: College of Health Sciences, University of Memphis, Memphis, Tennessee, United States of America

* Fabio.Demontis@stjude.org

Abstract

Myofiber atrophy occurs with aging and in many diseases but the underlying mechanisms are incompletely understood. Here, we have used >1,100 muscle-targeted RNAi interventions to comprehensively assess the function of 447 transcription factors in the developmental growth of body wall skeletal muscles in *Drosophila*. This screen identifies new regulators of myofiber atrophy and hypertrophy, including the transcription factor Deaf1. Deaf1 RNAi increases myofiber size whereas Deaf1 overexpression induces atrophy. Consistent with its annotation as a Gsk3 phosphorylation substrate, Deaf1 and Gsk3 induce largely overlapping transcriptional changes that are opposed by Deaf1 RNAi. The top category of Deaf1-regulated genes consists of glycolytic enzymes, which are suppressed by Deaf1 and Gsk3 but are upregulated by Deaf1 RNAi. Similar to Deaf1 and Gsk3 overexpression, RNAi for glycolytic enzymes reduces myofiber growth. Altogether, this study defines the repertoire of transcription factors that regulate developmental myofiber growth and the role of Gsk3/Deaf1/glycolysis in this process.

Author summary

Several diseases in humans reduce skeletal muscle mass and such wasting contributes to poor prognosis. Muscle mass is modulated in adulthood primarily by changes in the size of composing muscle cells (myofibers). Many of the signaling pathways that modulate myofiber size impinge on transcription factors. However, only few of the ~1,400 human transcription factors have been studied for their capacity to modulate skeletal muscle mass. To start to fill this gap in knowledge, we have used *Drosophila melanogaster* for testing the function of evolutionary conserved transcription factors. Because of the reduced genetic redundancy and the 40-fold increase in muscle mass that occurs in development, larval body wall skeletal muscles provide an ideal setting for identifying interventions that induce myofiber atrophy and hypertrophy. Here, we report the phenotype of >1,100

screen data is provided in S1 Table, the RNA-seq data is provided in S2 Table, and the phenotypes of RNAi lines for glycolytic enzymes are reported in S3 Table. Additional primary data, relative to Figs 2 and 3, are reported in S4 Table.

muscle-targeted RNAi interventions in myofiber size regulation. These include the transcription factor Deaf1, which induces hypertrophy upon RNAi and atrophy upon overexpression. These effects stem from modulation of glycolysis by Deaf1. Moreover, glycolysis is also modulated by the kinase Gsk3, which induces myofiber atrophy and muscle transcriptional changes similar to Deaf1. Altogether, our study provides a resource for understanding the function of 447 transcription factors in myofiber size regulation.

Introduction

Skeletal muscle is a key tissue of the human body accounting for approximately 40–50% of the total body mass. A balance between muscle protein synthesis and breakdown is essential for maintaining the functionality and size of skeletal muscles [1]. When muscle protein synthesis exceeds protein degradation, this leads to skeletal muscle hypertrophy, which typically results from an increase in myofiber size. Conversely, myofiber atrophy occurs when protein breakdown is excessive or protein synthesis is insufficient [1,2]. This occurs following inactivity, fasting, as a side effect of many pharmacological treatments, and in the course of many degenerative diseases such as cancer cachexia, chronic heart disease, diabetes, sepsis, infections, chronic obstructive pulmonary disease, and renal failure [3]. Importantly, the loss of muscle mass is not just a side-effect of these conditions but a rather important contributor to morbidity and mortality. Strikingly, prevention of skeletal muscle mass loss in tumor-bearing mice results in increased survival even if cancer progression is not halted [4–6]. Despite great strides towards understanding the mechanisms responsible for muscle wasting, incomplete knowledge in this area has hampered the development of suitable therapies.

Gene expression changes are fundamental drivers of myofiber atrophy [7]. Many signaling pathways that induce atrophy impinge on key transcription factors to promote muscle protein degradation [1,8–10]. For example, forkhead box O (FoxO) transcription factors are activated in response to decreased insulin/IGF signaling and induce the expression of components of the autophagy-lysosome and ubiquitin-proteasome systems which in turn mediate protein degradation [11–17]. However, apart from a few transcription factors that have been extensively studied [1,8], much remains to be learnt on the role that the ~1,400 transcription factors encoded by the human genome [18] play in skeletal muscle mass homeostasis.

Drosophila body wall skeletal muscles have emerged as an important model system to determine the mechanisms of muscle growth and differentiation [19–34]. Previously, we have found that FoxO overexpression in larval body wall skeletal muscles leads to myofiber atrophy and reduces developmental muscle growth [35], suggesting that the fruit fly *Drosophila melanogaster* can be used to identify evolutionary-conserved regulators of myofiber size [10,36,37]. Here, by examining the impact of transgenic RNAi on developmental muscle growth, we have tested 1,114 RNAi lines targeting 447 of the 708 transcription factors encoded by the *Drosophila* genome [38]. Our study provides information on many novel transcription factors necessary for myofiber size determination. These include the transcription factor Deaf1 that is annotated as a phosphorylation target of the kinase GSK3-b [39], which is a known inducer of atrophy [40,41]. Similar to Gsk3, Deaf1 overexpression induces myofiber atrophy, whereas Deaf1 RNAi induces myofiber hypertrophy. Gene expression profiling further indicates that Gsk3/Deaf1-induced changes in myofiber size are associated with corresponding changes in the expression of glycolytic enzymes. Altogether, this study expands the repertoire of transcription factors that are implicated in myofiber size determination and indicates a possible role of Deaf1 in this process.

Results

A RNAi screen targeting transcription factors in *Drosophila* body wall skeletal muscles identifies regulators of muscle atrophy and hypertrophy

Previously, it was found that novel regulators of myofiber size can be uncovered by testing their function in *Drosophila* body wall larval skeletal muscles. For example, the vast increase in muscle size (~40-fold) that occurs over ~5 days of *Drosophila* larval development is modulated by the insulin/Akt/TOR signaling pathway [35], which is a well-known modulator of atrophy and hypertrophy in mammals [1]. Moreover, loss of UBR4, a ubiquitin ligase implicated in atrophy-associated muscle proteolysis [42,43], induces hypertrophy in *Drosophila* and in mammals [37]. Altogether, these studies indicate that homologous signaling pathways modulate myofiber size in mammals and in the developing *Drosophila* larvae. Moreover, *Drosophila* body wall muscles constitute an excellent setup for the identification of transcription factors that regulate myofiber size, as found for FoxO and Mnt [35].

On this basis, we took advantage of the simplicity of this system and the availability of transgenic RNAi resources for tissue-specific modulation of gene function to interrogate the role of evolutionary-conserved transcription factors in myofiber size regulation. For these studies with UAS/Gal4, the skeletal muscle-specific *Mef2-Gal4* [44] was crossed with 1,114 transgenic RNAi lines (from the VDRC and Bloomington stock centers) to target 447 of the 708 transcription factors encoded by the *Drosophila* genome [38]. *Mef2-Gal4* drives transgene expression in the body wall musculature located beneath the epidermis, and composed of muscles with stereotypical sizes, each consisting of a single myofiber. Because skeletal muscle-specific interventions that regulate the size of body wall muscles correspondingly change the size of the larva [35,37], we have scored the size of larvae as a convenient readout to assess the outcome of muscle-specific RNAi interventions (Fig 1A).

Compared to control RNAi, ~88% RNAi interventions lead to 3rd instar larvae of normal size, indicating that these RNAi do not impact developmental muscle growth. However, there were RNAi interventions that lead to larval lethality (~1.6%) and various degrees of atrophy (~3.7%), indicating that transcription factors targeted by these RNAi are necessary for optimal skeletal muscle growth. Conversely, ~3% of RNAi lead to hypertrophy, indicating that the transcription factors targeted by these RNAi normally limit muscle growth. Additionally, there were ~3% of RNAi interventions that rather than affecting size primarily affected larval shape, leading to thin or sickle-shaped larvae (Fig 1B and S1 Table).

RNAi interventions that induce atrophy at the larval stage typically do not develop into adult flies [35]. Therefore, it is not surprising to find that ~16% of *Mef2-Gal4*-driven RNAi interventions did not yield any adults, as these include RNAi interventions that impact larval stages of muscle growth as well as pupal stages of muscle remodeling. However, there were some muscle-related phenotypes that were manifested in adult flies obtained from other RNAi crosses. These included early lethality of adult flies soon after eclosion, as well as defects in wing position. Normally, the wings are kept at stereotypical positions in adult flies but developmental defects that cause muscle degeneration lead to upheld and/or depressed wings, as found before for pink1/parkin loss [45] and here for ~1% of RNAi interventions that target transcription factors (Fig 1C and S1 Table). Altogether, by using muscle-restricted RNAi screening, we have here identified novel transcription factors that impact developmental skeletal muscle growth.

Among the many screen hits identified for their capacity to regulate myofiber size, there were 17 genes that scored consistently with 2 or more RNAi lines and that therefore are more likely to be robust regulators of muscle growth (S1 Table). To further test these genes, we re-screened them with *Mef2-Gal4* and also with an additional muscle-specific driver, *MhcK-Gal4*,
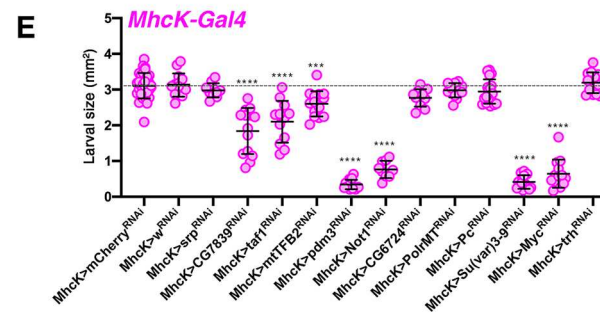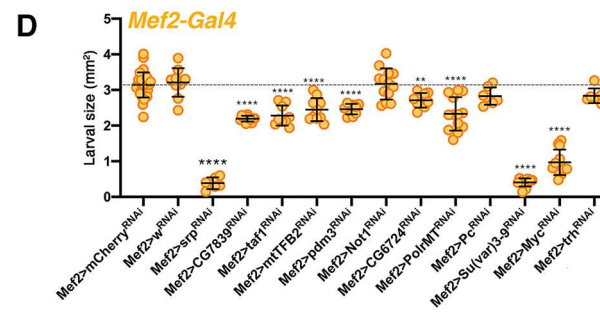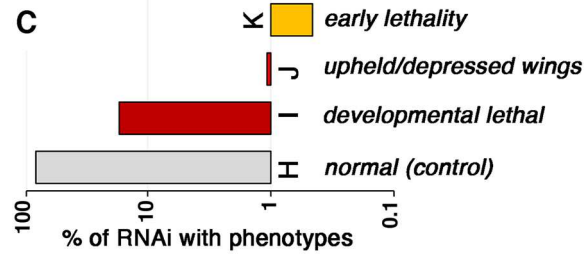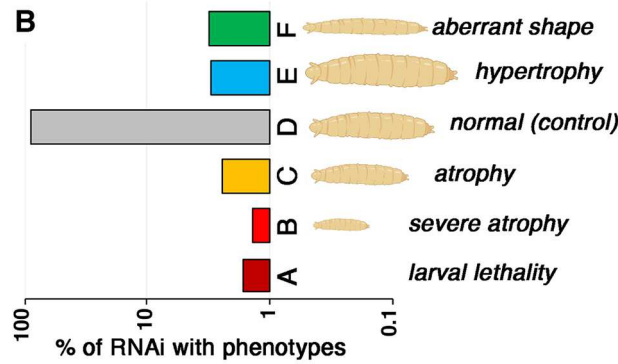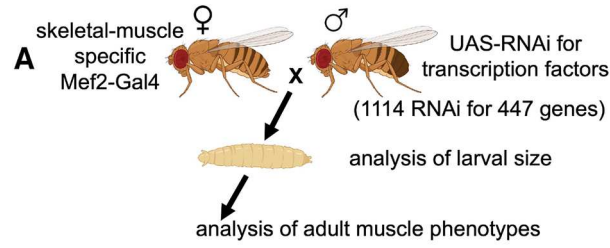
Fig 1. Muscle-specific RNAi screening identifies transcription factors that modulate developmental growth of *Drosophila* body wall skeletal muscles. (A) Scheme for the identification of transcription factors that modulate developmental skeletal muscle growth in *Drosophila*. The skeletal muscle-specific *Mef2-Gal4* was crossed with a collection of 1114 transgenic RNAi lines that target 447 transcription factors and transcriptional regulators to test their function in developmental muscle growth. *Mef-Gal4* drives transgene expression in the body wall musculature located beneath the epidermis, and composed of muscles with stereotypical sizes, each consisting of a single myofiber. Because skeletal muscle-specific interventions that regulate the size of body wall muscles correspondingly change the size of the larva [35,37], we have scored the size of larvae as convenient readout to assess the outcome of muscle-specific RNAi interventions. Moreover, in cases where adult flies eclosed, also wing positioning was scored as upheld or depressed wings can indicate muscle developmental defects and degeneration. (B) Compared to control RNAi, most RNAi interventions lead to 3rd instar larvae of normal size, indicating that these RNAi interventions do not impact developmental muscle growth. There were RNAi interventions that lead to larval lethality and various degrees of atrophy, indicating that transcription factors targeted by these RNAi are necessary for optimal skeletal muscle growth. Conversely, RNAi for another subset of transcriptional regulators lead to hypertrophy, indicating that the transcription factors targeted by these RNAi interventions normally limit muscle growth. Additionally, there were certain RNAi intervention that rather than affecting size primarily affected the shape of the larva, leading to thin or sickle-shaped larvae. (C) Although RNAi interventions that induce atrophy at the larval stage do not develop into adult flies, we have examined the adults that eclosed from all other RNAi interventions. The wings are kept at stereotypical positions in adult flies but developmental defects leading to muscle degeneration are known to lead to upheld and/or depressed wings, as found here for RNAi of several transcription factors. A full report of screen results is shown in S1 Table. (D-E) The area of larvae with muscle-specific expression of transgenic RNAi driven by *Mef2-Gal4* (D) and by *MhcK-Gal4* (E). Similar results are obtained with RNAi driven by both drivers, although some differences are found in the phenotypes induced by *Mef2-Gal4* versus *MhcK-Gal4*, presumably because of differences in the potency and tissue-specificity of these Gal4 lines. Mean±SD and N = 6–31 (D) and N = 9–32 (E) are shown; $^{**}P{<}0.01$, $^{***}P{<}0.001$, $^{****}P{<}0.0001$. The scheme in Fig 1 was drawn with BioRender.

https://doi.org/10.1371/journal.pgen.1009926.g001

which drives strong transgene expression from the embryonic stage of muscle development [46]. However, different from *Mef2-Gal4*, *InR* overexpression with *MhcK-Gal4* only marginally increased larval size (S1 Fig), suggesting that *MhcK-Gal4* might not be suitable to uncover muscle hypertrophy phenotypes compared to *Mef2-Gal4*. On this basis, we have re-screened with *MhcK-Gal4* only RNAi lines (from the Bloomington collection) with which we previously obtained a reduction in body size upon muscle-specific expression.

This follow-up analysis revealed that larval size is overall similarly affected by RNAi driven by *Mef2-Gal4* (Fig 1D) and by *MhcK-Gal4* (Fig 1E). However, some discrepancies in the phenotypes induced by *Mef2-Gal4* versus *MhcK-Gal4* were also observed, presumably because of differences in the potency and tissue-specificity of these Gal4 lines (Figs 1D–1E and S2). Specifically, RNAi for CG7839, taf1, mtTFB2, pdm3, Su(var)3-9, and myc (dm) consistently reduced larval body area with both *Mef2-Gal4* and *MhcK-Gal4*, although pdm3 RNAi yielded stronger effects with *MhcK-Gal4* versus *Mef2-Gal4*. However, RNAi for srp and PolrMT significantly reduced larval size with *Mef2-Gal4* but not with *MhcK-Gal4*. Moreover, RNAi for CG6724 marginally reduced larval size with both *Mef2-Gal4* and *MhcK-Gal4*, although this was statistically significant only with *Mef2-Gal4*. Conversely, RNAi for Not1 reduced larval size only when driven by *MhcK-Gal4*. Lastly, RNAi for Pc and tracheaeless (trh), which were previously classified as screen hits, did not significantly impact larval size when rescreened with *Mef2-Gal4* (Fig 1D), suggesting that they are false positives. Altogether, despite some differences, RNAi driven by *Mef2-Gal4* and *MhcK-Gal4* similarly impacts myofiber size (Fig 1D and 1E), indicating that our screen strategy is appropriate for finding candidate regulators of muscle growth.

The small set of high-confidence regulators of muscle growth includes genes with functional homologs in humans, i.e. CG7839/CEBPZ, taf1/TAF1, the mitochondrial transcription factor mtTFB2/TFB2M, pdm3/POU6F2, Su(var)3-9/SUV39H, and dm/MYC (Fig 1D and 1E and S1 Table). Although these transcription factors have not been previously implicated in muscle growth or wasting, apart dm/MYC [35], some were found to modulate muscle differentiation in mice. Specifically, TAF1 has been previously implicated in myogenesis via its

capacity to bind Pax3 and modulate its ubiquitination and proteasomal degradation [47] whereas the histone methyltransferase SUV39H1 was found to repress MyoD-stimulated myogenic differentiation [48].

Altogether, these findings indicate that RNAi screening in *Drosophila* is a useful approach to identify novel candidate regulators of myofiber size determination.

Muscle-specific RNAi for screen hits identifies transcription factors that modulate developmental myofiber growth in *Drosophila*

We have conducted a large-scale RNAi screen for transcription factors that regulate developmental skeletal muscle growth in *Drosophila*. Because body wall skeletal muscles are located beneath the epidermis, genetic interventions that regulate muscle size correspondingly change the size of the larva [35,37]. Assessing larval size is an easily-scorable screen readout that has led to the identification of many regulators of developmental muscle growth (Fig 1).

To better test the impact of screen hits, we have determined their impact on myofiber size via larval dissections and analysis of body wall skeletal muscles. Specifically, the outcome of some muscle-specific interventions that affected larval size was validated via the analysis of a set of representative muscles, ventral longitudinal VL3 and VL4 muscles, which are each composed by a single myofiber with a stereotypical size [35,37].

For these studies, we selected a set of genes based on their extremely high evolutionary conservation (i.e., typically, a DIOPT score >7), consistent scoring with multiple RNAI lines, and/or novelty (Fig 2 and S1 Table). Compared to controls (white^{RNAi} and mcherry^{RNAi}), RNAi for screen hits driven in skeletal muscle by *Mef2-Gal4* led to decreased (atrophy) and increased (hypertrophy) size of VL3 and VL4 skeletal muscles. Quantification of the cumulative area of VL3 and VL4 muscles from multiple larvae indicates that RNAi for Nurf-38, e(y)1, alien, CG7839, Taf1, MBD-R2, mtTFB2, pdm3, and dati reduces VL3+VL4 muscle area (atrophy). This indicates that these transcription factors are necessary for optimal myofiber growth during larval development. Conversely, muscle-specific RNAi for FoxO, Cnc, and Deaf1 increases the area of VL3+VL4 muscles (hypertrophy), indicating that these transcription factors normally limit developmental myofiber growth. Altogether, these histological analyses confirm that this muscle-targeted RNAi screen has identified novel transcription factors that regulate myofiber developmental growth.

Deaf1 RNAi induces myofiber hypertrophy whereas Deaf1 overexpression causes myofiber atrophy

Among the many regulators of skeletal muscle homeostasis identified in this screen, RNAi interventions that induce myofiber hypertrophy are the most interesting as they highlight transcription factors that normally impede growth and that could be inhibited to contrast wasting. Among them, the transcription factor Deaf1 (deformed epidermal autoregulatory factor 1) has been previously implicated in early development and innate immunity in *Drosophila* [49–52] and in human neurodevelopmental disorders [53–55] but not in muscle growth. On the basis of this possible novel function of Deaf1 in muscle, we further examined its impact on myofiber size determination. Whereas Deaf1 RNAi induces hypertrophy compared to control RNAi (Fig 2D), muscle-restricted Deaf1 overexpression led to myofiber atrophy (Fig 3A). Specifically, the area of ventral longitudinal VL3 and VL4 muscles is lower upon *Deaf1* overexpression (Fig 3B), whereas it increases upon *insulin receptor* (*InR*) overexpression, as expected [35].
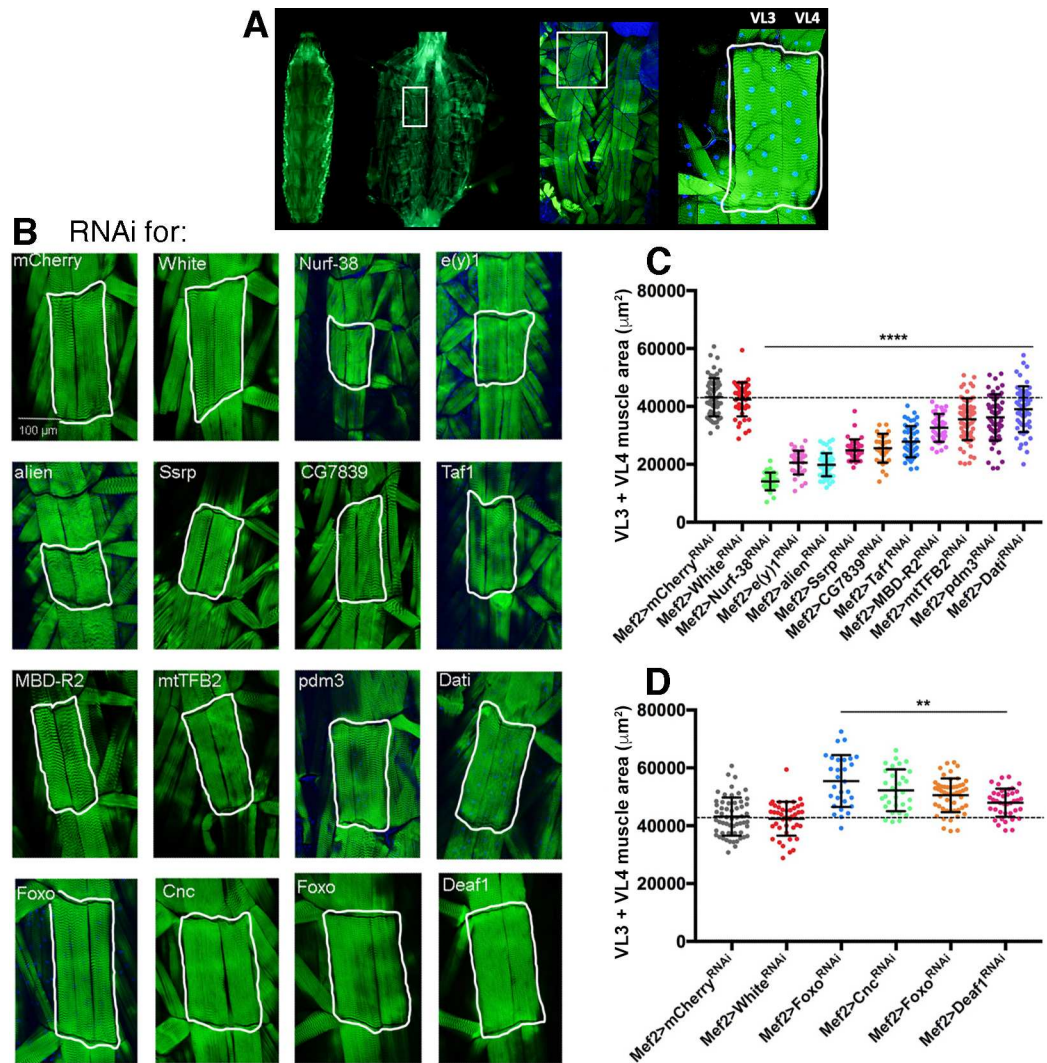
Fig 2. Muscle-specific RNAi for screen hits identifies transcription factors that modulate developmental myofiber growth in *Drosophila*. (A) Validation of RNAi screen hits via dissection of 3rd instar larvae and confocal imaging of ventral longitudinal VL3 and VL4 body wall skeletal muscles, which have stereotypical sizes. (B) Compared to controls (white^RNAi and mcherry^RNAi), RNAi for screen hits driven in skeletal muscle by *Mef2-Gal4* leads to a decrease (atrophy) and an increase (hypertrophy) in the size of VL3 and VL4 skeletal muscles, each consisting of a single myofiber. (C) Quantitation of the cumulative area of VL3 and VL4 muscles from multiple larvae indicates that RNAi for Nurf-38, e(y)1, alien, CG7839, Taf1, MBD-R2, mtTFB2, pdm3, and Dati reduces VL3+VL4 muscle area (atrophy). This indicates that these transcription factors are necessary for optimal myofiber growth during larval development. (D) Conversely, muscle-specific RNAi for Foxo, Cnc, and Deaf1 increases the area of VL3+VL4 muscles (hypertrophy), indicating that these transcription factors limit developmental myofiber growth. N = 12–70 and mean±SD is shown; **$P<0.01$, ***$P<0.001$.

Gsk3 regulates myofiber size similar to Deaf1

Although Deaf1 has not been implicated in myofiber size determination, it was previously identified as a phosphorylation target of the glycogen synthase kinase GSK3 [39], which induces myofiber atrophy and muscle wasting in response to many catabolic stimuli via the phosphorylation of target proteins in mice [14,41,56]. Specifically, it was found that DEAF1 interacts with and is phosphorylated by GSK3A and GSK3B [39]. To determine whether shaggy (the Drosophila homolog of GSK3 and GSK3B) regulates myofiber size in Drosophila as found in mammals, we modulated its activity via overexpression of constitutive active
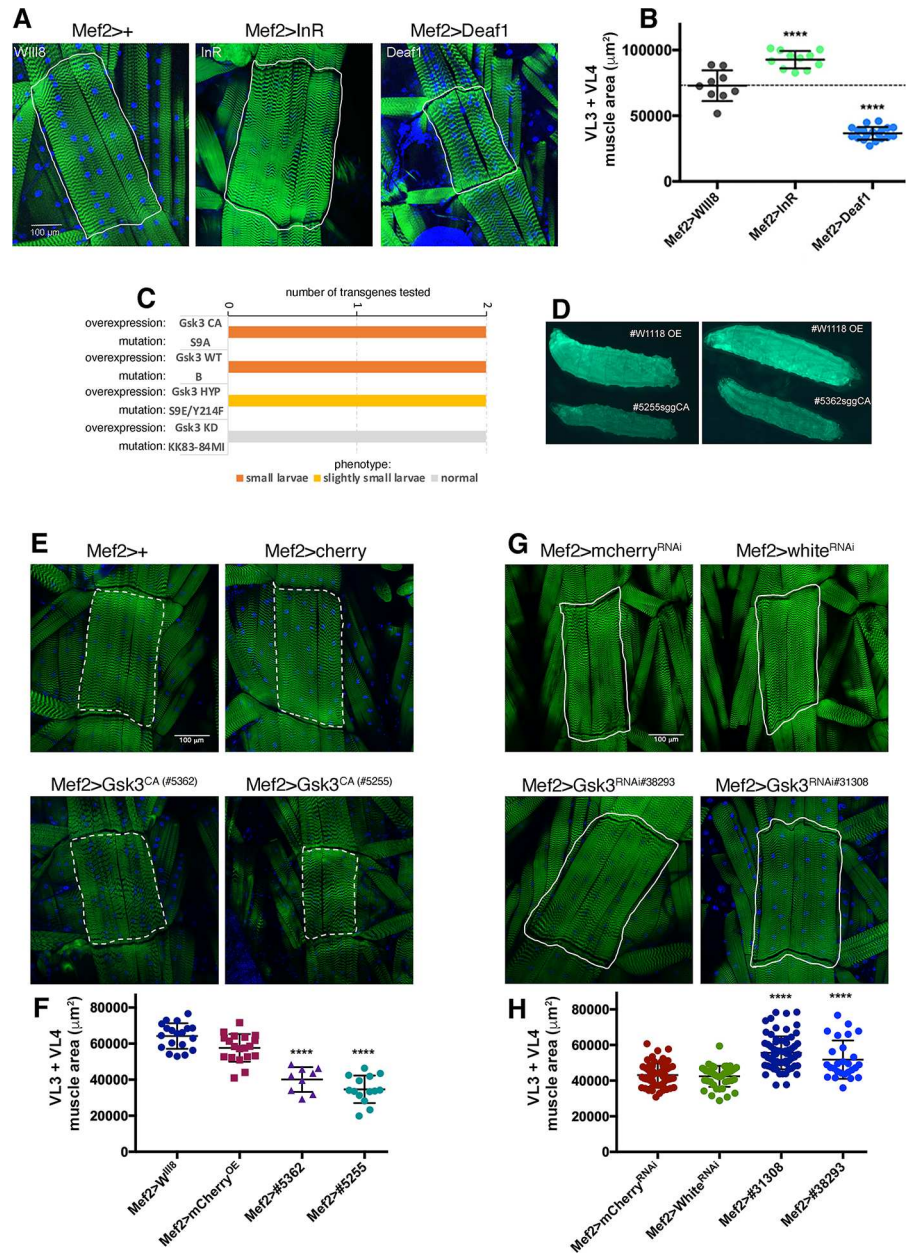
Fig 3. Muscle-restricted activity of Deaf1 and Gsk3 impedes developmental muscle growth. (A) Transgenic overexpression of the transcription factor *Deaf1*, driven specifically in skeletal muscle with *Mef2-Gal4*, leads to a reduction in the area of larval muscles, each consisting of a single myofiber, compared to controls with no transgene expression (*Mef2>+*). (B) The area of ventral longitudinal VL3 and VL4 muscles is lower upon *Deaf1* overexpression, whereas it increases upon *insulin receptor* (*InR*) overexpression. N = 9–19 and mean±SD is shown; $^{****}P < 0.001$. (C) Gsk3 transgenic overexpression driven in skeletal muscle with Mef2-Gal4 leads to small size of 3rd instar larvae in a manner proportional to Gsk3 kinase activity: Gsk3 CA (constitutive active) and WT (wild-type) induce atrophy, hypomorphic (HYP) mutants with only limited kinase activity have little impact, whereas KD (kinase-dead) Gsk3 mutants do not affect developmental muscle growth. (D) Gsk3 activity in muscle reduces body size, as indicated by larvae where body wall skeletal muscle are shown by expression of Mhc-GFP. (E) Compared to controls (no transgene and *mcherry* overexpression), overexpression of 2 different *Gsk3^CA* transgenes with *Mef2-Gal4* leads to a decrease (atrophy) in the size of myofibers, as indicated by the quantitation of the cumulative area of VL3 and VL4 muscles from multiple larvae (F); N = 9–19 and mean±SD is shown; $^{****}P < 0.0001$. (G) Conversely, Gsk3 RNAi in skeletal muscle induces myofiber hypertrophy, as indicated by the the cumulative area of VL3 and VL4 muscles (H); N = 27–71 and mean±SD is shown; $^{****}P < 0.0001$.

versions. Specifically, we employed *Mef2-Gal4* to drive expression of transgenes encoding for constitutive-active, wild-type, and kinase-dead Gsk3. As expected based on its function in higher organisms, we found that muscle-specific overexpression of constitutive active (CA) and wild-type (WT) *Gsk3* led to reduced body size, which is indicative of muscle atrophy (Fig 3C and 3D). On the other hand, Gsk3 variants with reduced kinase activity minimally impacted larval size, and kinase-dead Gsk3 mutants had no effect (Fig 3C and S3 Table).

To corroborate these findings, larvae with skeletal muscle-specific *Gsk3*[CA] overexpression were dissected and the area of ventral longitudinal VL3 and VL4 muscles analyzed. As expected based on the function of Gsk3 in mammalian systems [14,41,56] and our preliminary analyses (Fig 3C and 3D), Gsk3[CA] lead to significant decline in myofiber size (Fig 3E and 3F). To further assess the role that Gsk3 plays in *Drosophila* body wall muscle growth, we reduced its levels in skeletal muscle via RNAi. Conversely to Gsk3 activation (Fig 3C–3F), Gsk3 RNAi induced myofiber hypertrophy, compared to control RNAi lines against *white* and *mcherry* (Fig 3G and 3H).

Altogether, these findings indicate that Gsk3, similar to Deaf1, regulates muscle mass in *Drosophila* (Fig 3), as observed in mammals [14,41,56]. Because Deaf1 was found to be a phosphorylation target of Gsk3 [39], these findings suggest that Deaf1 may negatively regulate myofiber size in *Drosophila* skeletal muscle by acting downstream of Gsk3 signaling.

Gsk3 and Deaf1 induce similar gene expression changes in *Drosophila* body wall skeletal muscles

Because the transcription factor DEAF1 has been previously reported to interact with and to be phosphorylated by GSK3A/B [39], and it similarly regulates myofiber size (Fig 3), we next examined whether Gsk3 and Deaf1 induce similar gene expression changes in *Drosophila* body wall skeletal muscle. For these studies, we used *Mef2-Gal4* to modulate the levels of Deaf1 and Gsk3 in muscle. As expected, Deaf1 mRNA levels were significantly lower upon Deaf1 RNAi and higher upon Deaf1 overexpression, respectively. Similarly, higher Gsk3 levels were found upon its overexpression (Fig 4A).

RNA sequencing from filleted larvae (which consist primarily of body wall skeletal muscles and the associated epidermis) identified many transcriptional changes that occur upon Deaf1 RNAi in comparison to control white RNAi. Cross-comparison with gene expression changes induced by *Deaf1* overexpression revealed that significantly regulated genes (p<0.05) are largely regulated in opposite fashions by Deaf1 RNAi and Deaf1 overexpression ($R^2 = 0.46$), each normalized to its respective control (Fig 4B). Moreover, comparison of the muscle transcriptomes revealed that gene expression changes induced by *Deaf1* overexpression are highly overlapping ($R^2 = 0.49$) with those induced by constitutive active Gsk3 (Fig 4C).

GO term analysis of categories enriched among genes upregulated by Deaf1 RNAi indicates that Deaf1 RNAi may induce myofiber hypertrophy by promoting glycolysis, sarcomere organization, and by modulating the function of histone deacetylases (Fig 4D). In particular, glycolysis represents the top category of genes upregulated by Deaf1 RNAi and, consistent with transcriptome cross-comparisons (Fig 4B and 4C), Deaf1 and Gsk3 overexpression induce converse changes, i.e. significantly reduce expression of most glycolytic enzymes (Fig 4E). Altogether, these findings suggest that the transcription factor Deaf1 may regulate myofiber size via the transcriptional modulation of several target genes, including glycolytic enzymes.

Expression of glycolytic enzymes sustains growth of larval body wall skeletal muscles

We have found that Deaf1 RNAi, which induces myofiber hypertrophy, promotes the expression of glycolytic enzymes whereas Deaf1 overexpression, similar to Gsk3, reduces their

A

B

p<0.05
R²=0.4603

C

p<0.05
R²=0.4967

Logratio Deaf1 OE / nc (x axis)
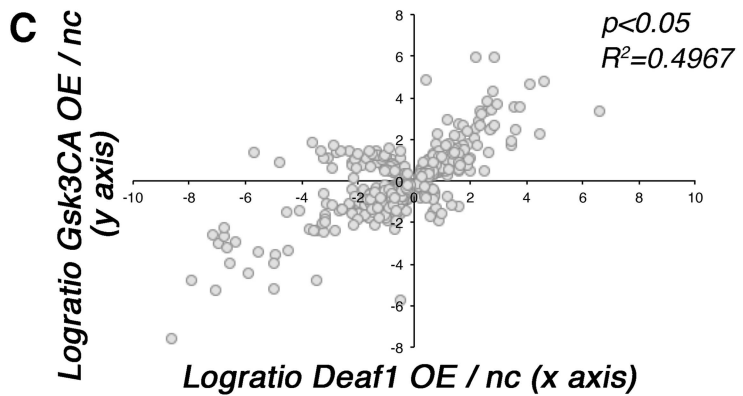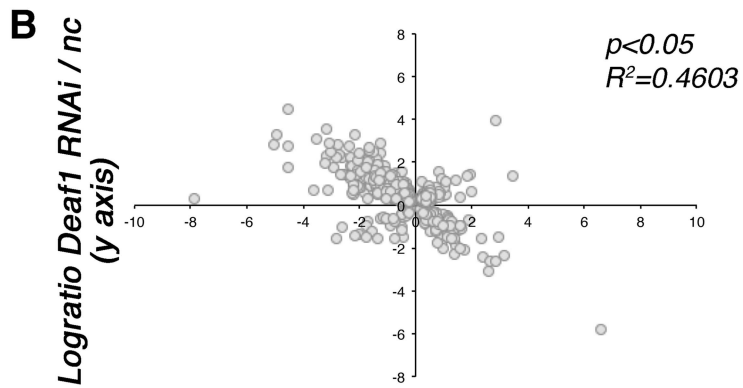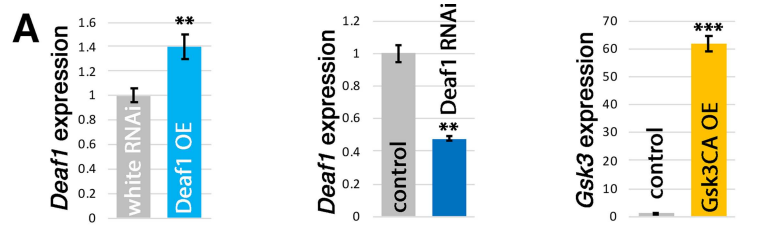
D **Upregulated genes by Deaf1 RNAi (GO terms)**
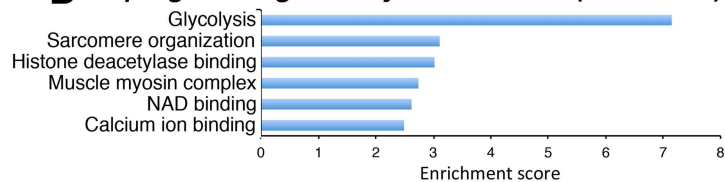
E

GLYCOLYSIS	Deaf1 OE / nc	Deaf1 RNAi / nc	Gsk3CA OE / nc
Hex-A	-0.38	0.17	-1.43
Pgi	-1.61	1.15	-1.77
Pfk	-1.58	1.51	-1.08
Ald	-1.75	1.27	-1.65
Tpi	-1.5	1.44	-1.11
Gapdh1	-1.63	1.42	-1.61
Gapdh2	-1.59	1.05	-1.38
Pgk	-0.97	1.11	-1.09
Pglym78	-1.38	1.23	-1.34
Eno	-1.31	1.67	-1.37
PyK	-1.42	1.4	-1.43

UPREGULATED

DOWNREGULATED

NOT SIGNIFICANTLY REGULATED

Fig 4. GSK3 and Deaf1 induce similar gene expression changes in larval skeletal muscles. (A) Validation of genetic interventions. Muscle-restricted *Deaf1* overexpression leads to an increase in Deaf1 mRNA levels, opposite to Deaf1 RNAi. As expected, GSK3 overexpression also increases Gsk3 mRNA levels. (B) Coincident with their opposite roles in regulating myofiber size, converse gene expression changes ($R^2 = 0.46$; genes regulated with $p<0.05$) are induced in larval body wall muscles by Deaf1 overexpression (OE) and Deaf RNAi, each normalized to their respective controls, i.e. no transgene overexpression and control white RNAi. (C) Largely similar gene expression changes are induced by overexpression of Deaf1 and of constitutive active (CA) Gsk3 ($R^2 = 0.49$; $p<0.05$). (D) DAVID GO term analysis reveals gene categories that are enriched among Deaf1-regulated genes, which include glycolysis. (E) Analysis of glycolytic genes reveals that most of them are significantly ($p<0.05$) and concordantly regulated by Deaf1 and Gsk3. Specifically, glycolytic enzymes are upregulated by Deaf1 RNAi compared to control whereas their expression is suppressed by Deaf1 OE and Gsk3CA OE. S2 Table reports the results of RNA sequencing.

expression (Fig 4). On this basis, we next tested the impact of glycolysis on skeletal muscle growth. To this purpose, we screened 44 RNAi lines targeting glycolytic enzymes with *Mef2--Gal4* and found that many of them led to small larval size (Fig 5A and S3 Table), indicative of muscle atrophy [35]. We further analyzed some of the RNAi lines that target glycolytic enzymes. As expected, small body size due to expression of transgenic RNAi for *Eno* and *Pglym78* in skeletal muscle (Fig 5A) was associated with reduced size of VL3 and VL4 muscles (Fig 5B and 5C). These findings indicate that glycolysis is necessary for myofiber growth, in line with previous studies [57,58], and that it may indeed be a primary means by which Gsk3 and Deaf1 modulate myofiber growth in *Drosophila* body wall skeletal muscles.

Discussion

In this study, we took advantage of a simple, genetically tractable, model organism, *Drosophila melanogaster* [59], to expand the knowledge about transcription factors that regulate myofiber size. Specifically, we have used transgenic RNAi to knock down the levels of evolutionary-conserved transcription factors in *Drosophila* larval body wall skeletal muscles which, by growing ~40-fold during few days of larval development, offer an ideal setup for identifying modulators of myofiber growth. Because these muscles are located right beneath and surround the larval epidermis, changes in muscle mass result in changes in the overall larval body size, making this system amenable for visual phenotypic screens [35,37]. Moreover, the reduced genetic redundancy of *Drosophila melanogaster* compared to mice and humans constitutes another advantage for uncovering regulators of myofiber size [22], as demonstrated by the lower number of transcription factors present in *Drosophila* compared to humans (708 versus ~1,400).

The RNAi screen here done provides insight into transcription factors that regulate myofiber growth. Because this screen included both DNA-binding transcription factors and transcriptional regulators that are part of larger nuclear complexes, we expect that the screen hits here identified may modulate myofiber size via a plethora of mechanisms. For example, the nucleosome remodeling factor Nurf-38 catalyzes ATP-dependent nucleosome sliding and facilitates transcription of chromatin [60] and this may constitute a mechanism by which it is necessary for myofiber growth. Another example is e(y)1/Taf9, i.e. TBP-associated factor 9, which encodes for a component of the transcription factor IID complex, which regulates transcription from core promoters and enhancer-promoter interactions [61] but also regulates lipid metabolism [62], which has been implicated in muscle wasting [63]. Overall, despite phenotypic similarity, the transcription factors and transcriptional regulators here identified may regulate myofiber size via distinct target genes and transcriptional/chromatin remodeling mechanisms.

The RNAi screen we have conducted has identified several candidate regulators of muscle growth. However, as found in other screens [64], some of these hits could be false positives. For example, *tracheless (trh)*, a transcription factor necessary for the development of the
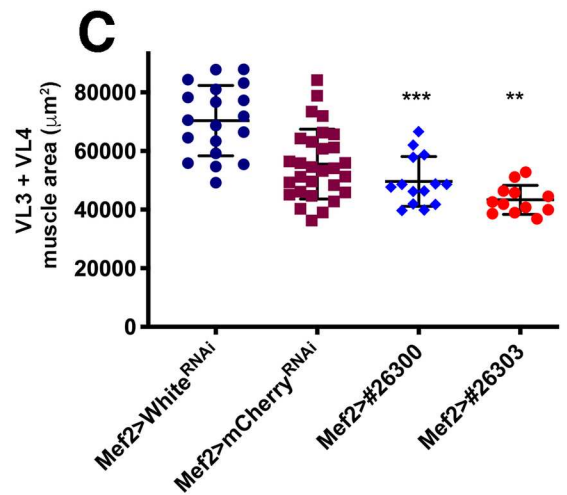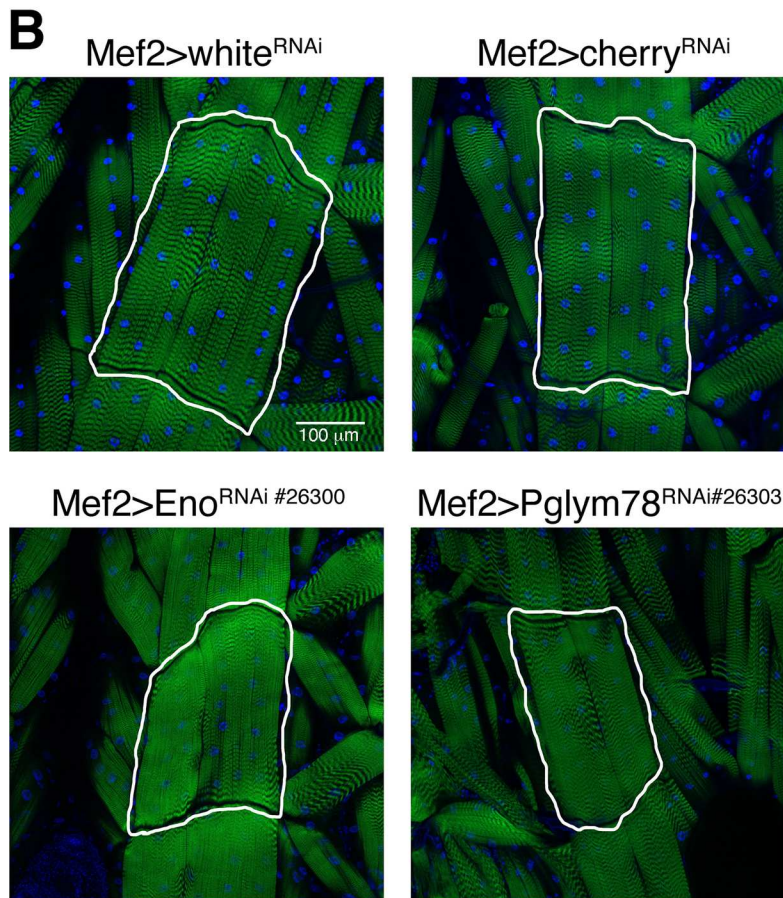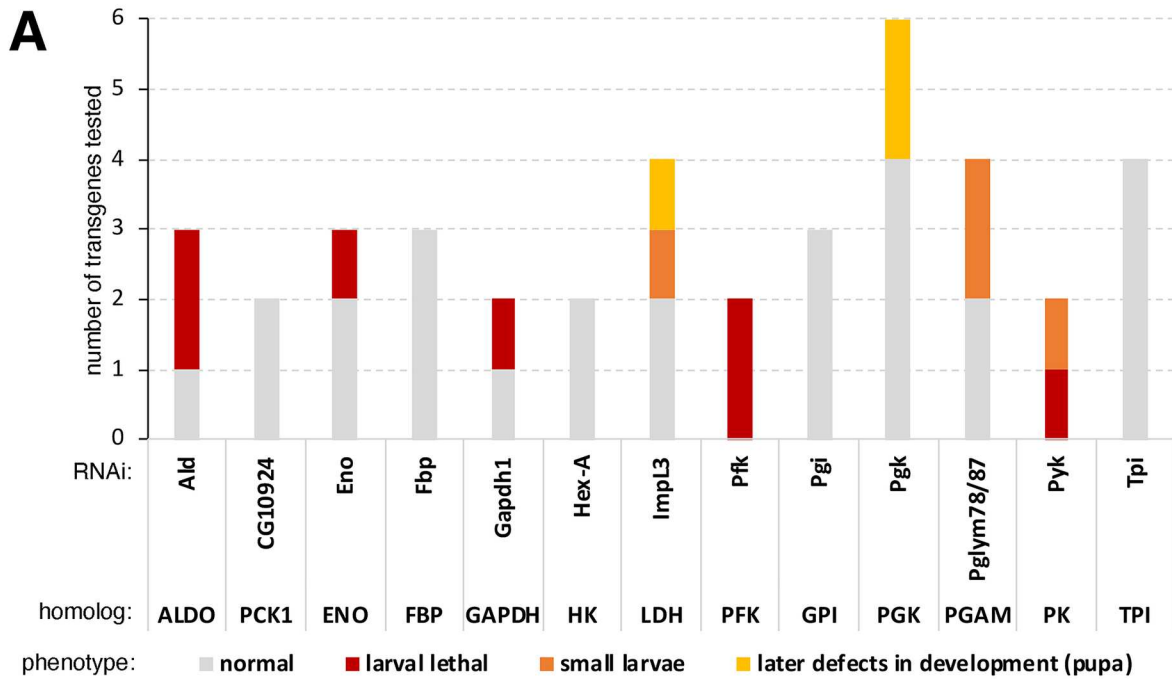
Fig 5. RNAi for glycolytic enzymes impedes developmental growth of larval body wall skeletal muscles. (A) RNAi for glycolytic enzymes driven in skeletal muscle with Mef2-Gal4 leads to small size of 3rd instar larvae, indicating that glycolysis is needed to sustain developmental muscle growth. A full list of phenotypes obtained with 44 lines targeting glycolysis is reported in S3 Table. (B) Transgenic RNAi for the glycolytic enzymes *Eno* and *Pglym78* reduces myofiber size, compared to control white[RNAi] and cherry[RNAi]. (C) The area of ventral longitudinal VL3 and VL4 muscles, each consisting of a single myofiber, is reduced upon Eno[RNAi] and Pglym78[RNAi]. N = 12–29 and mean±SD is shown; **$P<0.01$ and ***$P<0.001$.

https://doi.org/10.1371/journal.pgen.1009926.g005

Drosophila airway system [65], was initially identified as a screen hit but subsequent re-testing with *Mef2-Gal4* uncovered only minor phenotypes induced by trh RNAi (Fig 1D), suggesting that this is a false positive. While transcription factors that scored consistently with multiple RNAi lines (such as Deaf1 RNAi) are less likely to be false positives, screen hits identified with a single RNAi line most likely also consist in large part of bona fide muscle growth regulators (indeed in some cases only a single RNAi line was available to test the function of a given transcription factor).

Conversely, other transcription factors that are important regulators of muscle growth may not have scored because of technical limitations, i.e. they could be false negatives. Although the potency of transgenic RNAi depends on the Gal4 line used and specific RNAi collection, a previous study in the *Drosophila* embryo has found that phenotypes were observed only among the RNAi interventions that yielded a target gene knockdown greater than 50% [66]. Specifically, this study has found that, out of ~450 RNAi lines targeting kinases, ~29% were not functional (~12% did not display any knockdown, and an additional ~17% displayed a knockdown of less than 50% that did not yield a phenotype; [66]). Therefore, it is possible that around 1/3 of the lines tested in our screen is not functional and that therefore the muscle growth regulators targeted by these RNAi lines are not uncovered by our screen. On this basis, rather than being an exhaustive and definitive determination of the transcription factors that regulate muscle growth, our study provides a list of candidate regulators of myofiber size which should be further tested in *Drosophila* and other model organisms.

Another limitation of the screen consists in the tissue specificity of the *Mef2-Gal4* line that we have used. As originally described in ref. [35], this *Mef2-Gal4* line drives transgene expression in body wall skeletal muscles but also in visceral muscles and in some cells in the brain [35]. Closer analysis of such brain cells suggests that they consist of mushroom body neurons (S2 Fig), which have been found to express endogenous *Mef2* [67]. However, *Mef2-Gal4* fluorescence is most strongly observed in skeletal muscle compared to non-muscle cells and therefore it is unclear if sufficient target gene knockdown is achieved in non-muscle cells to generate a phenotype. Moreover, the overall similarity of phenotypes induced by transgenic RNAi driven by complementary muscle drivers (i.e. *Mef2-Gal4* and *MhcK-Gal4*) suggests that the observed muscle atrophy phenotypes are indeed due to RNAi expression in skeletal muscle (Fig 1D and 1E). Nonetheless, the changes in larval body size and myofiber growth observed in our study may in some cases depend on the modulation of the target gene outside of skeletal muscle. As in the case of false and negative screen hits, this constitutes a technical limitation of the study that will be resolved by complementary approaches for testing the function of the candidate regulators of myofiber size here identified.

Among the many screen hits identified, we have examined in more detail the function of Deaf1, an evolutionary conserved transcription factor that had not been previously implicated in skeletal muscle growth. Specifically, we have found that Deaf1 RNAi induces myofiber hypertrophy whereas Deaf1 overexpression causes atrophy. Mechanistically, Deaf1 RNAi promotes the expression of glycolytic enzymes whereas Deaf1 overexpression reduces it, suggesting that glycolysis is necessary for optimal skeletal muscle growth, as previously found in *Drosophila* [57] and in other contexts [68].

We also find that similar transcriptional responses, including expression of glycolytic enzymes, are induced by Deaf1 and Gsk3, a known inducer of myofiber atrophy [40,69–71] that interacts with and phosphorylates Deaf1 [39]. Many phosphorylation targets of GSK3 have been identified in mammals, including several transcription factors, such as MITF, NF-κB, and CREB [72–77]. However, much remains to understand about the GSK3 targets that are most necessary for GSK3 output in distinct tissues and disease conditions. In particular, although it is well established that GSK3 promotes muscle wasting [40,69–71], it is incompletely understood how GSK3 promotes transcriptional changes that drive muscle protein catabolism during atrophy. Our findings now suggest that Deaf1 may contribute at least in part to the transcriptional changes induced by Gsk3 activity in muscle, and that these may include the modulation of glycolysis.

Altogether, this study has expanded the repertoire of transcription factors that regulate myofiber growth and highlights a possible role for Gsk3, Deaf1, and glycolysis in this process.

Materials and methods

RNAi screening

The list of fly stocks used for RNAi screening is reported in S1 Table and refers to RNAi for *Drosophila* transcription factors that are evolutionarily conserved in humans, as defined based on a homology DIOPT [78] score of ≥2. For each screen cross, 10 *Mef2-Gal4* virgin females were crossed with 5 males for each RNAi line tested. Progenies were reared at 25˚C and transferred to new food every 4 days. Subsequently, the size of 3rd instar wandering larvae was scored in comparison with negative controls (white[RNAi]) and positive controls, which consisted in *FoxO* overexpression (which induces atrophy) and overexpression of *insulin receptor* (InR, which induces hypertrophy), as previously shown [35,37]. Specifically, larval size phenotypes due to *Mef2-Gal4*-driven RNAi in muscle were scored as follows: A- no larvae/no pupae; B- very small larvae/no pupae (i.e. smaller than *FoxO* overexpression); C- small larvae/small pupae (i.e. similar to *FoxO* overexpression); D- normal (no visible phenotype); E- increased larval/pupal size (i.e. similar to *InR* overexpression); and F- thin or sickle-shaped larvae with locomotor defects.

Adult flies obtained from RNAi crosses were scored based on the following categories: H-normal; I- no adults eclosed, i.e. developmental lethal; J- upheld or depressed wings in the majority of flies in the tube (i.e. similar to pink1 RNAi or parkin RNAi); and K- early lethality of eclosed flies. Normal muscle development results in stereotypical wing positioning, which is present in white[RNAi] control flies, whereas upheld/depressed wings are an indication of improper muscle development and/or muscle degeneration [45]. RNAi interventions that lead to small larvae and pupae (A-C) and larvae with aberrant shape (F) typically do not give rise to adult flies, as previously shown [35].

Drosophila stocks

In addition to *Mef2-Gal4* [44], the following fly stocks were used: UAS-Deaf1 [50], UAS-foxo and UAS-InR [35,79], and stocks for overexpression of wild-type, constitutive-active, and kinase-dead Gsk3 transgenes [80], which are reported in S3 Table. MhcK-Gal4 (Mhc-GAL4.K, BL#55133; [46]) was used for studies in Fig 1E. The list of fly stocks used for RNAi screening is reported in S1 Table whereas the list of RNAi lines that target glycolytic enzymes is reported in S3 Table.

The fly stocks utilized for VL3+VL4 muscle analyses (Fig 2) are the following: UAS-white-[RNAi] (BL#33623), UAS-cherry[RNAi] (BL#35785), UAS-Nurf-38[RNAi] (BL#31341), UAS-e(y)1[RNAi] (BL#32345), UAS-alien[RNAi] (BL#28908), UAS-Ssrp[RNAi] (BL#26222), UAS-CG7839[RNAi]

(BL#25992), UAS-Taf1[RNAi] (BL#32421), UAS-MBD-R2[RNAi] (BL#27029), UAS-mtTFB2[RNAi] (BL#27055), UAS-pdm3[RNAi] (BL#35726), UAS-dati[RNAi] (BL#26711), UAS-foxo[RNAi] (BL#27656 and BL#32993), UAS-Cnc[RNAi] (BL#32863), and UAS-Deaf1[RNAi] (BL#32512).

The fly stocks utilized for RNA-seq (Fig 4) are the following: UAS-Deaf1[RNAi] (BL#32512), UAS-white[RNAi] (BL#33623), UAS-Deaf1 [50], UAS-Gsk3[CA] (BL#5255), and w[1118] (+).

Staining of body wall skeletal muscles, confocal microscopy, and image analysis

Male larvae were dissected in ice-cold Ca^{2+}-free, $MgCl_2$-free PBS (Gibco) and filleted larval samples were fixed for 20 minutes in PBS with 4% paraformaldehyde, as previously done [35]. After washing with PBS, body wall skeletal muscles were stained overnight with DAPI (4',6-diamidino-2phenylindole, 1μg/mL) to visualize nuclei, and imaged to detect the endogenous fluorescence of a Mhc-GFP fusion protein. Body wall muscles were mounted on microscope slides and the VL3/4 muscles were imaged using a Zeiss LSM880 confocal laser-scanning microscope. Confocal images were analyzed using the measure tools of the ImageJ software to quantitate the area of VL3+VL4 muscles for each sample. Larval body size was quantified with ImageJ.

RNA sequencing

RNA-seq was done following similar procedures as before [81,82]. Specifically, total RNA was extracted from filleted *Drosophila* larvae, which consist primarily of body wall skeletal muscles. Three biological replicates were prepared for RNA-seq with the TruSeq stranded mRNA library preparation kit (Illumina) and sequenced on the Illumina HiSeq 4000 platform, with six samples in each lane. Multiplexing was done on a per flowcell basis. Approximately 100 million reads were obtained for each sample. FASTQ sequences derived from mRNA paired-end 100-bp sequences were mapped to the *Drosophila melanogaster* genome (BDGP5) with the STAR aligner (version 2.5.3a) [83]. Transcript level data were counted using HTSeq (version 0.6.1p1) [84] based on the BDGP5 GTF release 75. The TMM method [85] was used to calculate the normalization factors. Then, linear modeling was carried out on the log2(CPM) (count per million) values where the mean-variance relationship is accommodated using precision weights calculated by the voom function [86] of the limma package in R 3.2.3 (R Core Team 2013; [87]). A q-value (FDR) was calculated for multiple comparison adjustments of RNA-seq data. The lmFit, eBayes, and contrasts.fit functions from the limma package were used for the linear modeling. Statistical analyses were performed using log2(FPKM) values in Partek Genomic Suite 6.6 (www.partek.com/partek-genomics-suite/). The gene sets were analyzed by DAVID (Database for Annotation Visualization and Integrated Discovery) to identify enriched functional classes of genes [88].

The RNA-seq comparisons refer to *Mef2>Deaf1RNAi(BL#32512)* versus *Mef2>whiteRNAi (BL#33623)*, *Mef2>Deaf1* versus *Mef2>+*, and *Mef2>Gsk3CA(BL#5255)* versus *Mef2>+*; (n = 3/genotype). The RNA-seq data is reported in S2 Table and has been deposited to the Gene Expression Omnibus with accession number GSE174637.

Statistical analysis

All data points refer to biological replicates and the number is indicated in the figure legends. Each biological replicate refers to data obtained from a different larva; typically, larvae from 2 or more crosses were analyzed for each genotype. The larvae analyzed in Figs 2–5 were obtained from crosses different from those used for the screen. The unpaired two-tailed Student's t-test was used to compare the means of two independent groups to each other. One-

way ANOVA with Tukey's post hoc test was used for multiple comparisons of more than two groups of normally distributed data. Bar graphs present the mean ± SEM or ± SD, as indicated in the figure legends. Throughout the figures, asterisks indicate the significance of the p value: $^*p<0.05$; $^{**}p<0.01$; $^{***}p<0.001$. A significant result was defined as $p<0.05$. Statistical analyses were done with Excel and GraphPad Prism.

Supporting information

S1 Fig. Comparison of *Insulin Receptor* overexpression with *Mef2-Gal4* and *MhcK-Gal4*. Consistent with previous studies in *Drosophila* and mammals, overexpression of *insulin/IGF receptor* (*InR*) in skeletal muscle via *Mef2-Gal4* induces skeletal muscle hypertrophy, as indicated by the increase in body size. However, a relatively minor increase is found with *InR* overexpression via *MhcK-Gal4* (Mhc-Gal4.K, BL#55133) suggesting that this Gal4 line is not ideal for uncovering muscle hypertrophy phenotypes.
(TIF)

S2 Fig. Characterization of the tissue-specificity of transgenic expression with *Mef2-Gal4*. Red fluorescence due to transgenic *DsRed* expression is detected primarily in body wall skeletal muscles but also in visceral muscles and few cells in the brain. We find no evidence for *Mef2-Gal4*-driven *DsRed* expression in insulin producing cells (ipc) with this line. However, *DsRed* expression driven by *Mef2-Gal4* is detected in brain cells of the mushroom body (mb), consistent with our original characterization of this driver (Demontis and Perrimon, 2009, *Development*; PMID:*19211682*) and a more recent study that has found endogenous *Mef2* expression in a subset of Kenyon cells of the mushroom body (Crittenden et al. 2018, *Biology Open*; PMID:*30115617*).
(TIF)

S1 Table. RNAi screen data.
(XLSX)

S2 Table. RNA-seq data.
(XLSX)

S3 Table. Phenotypes of RNAi lines for glycolytic enzymes.
(TIF)

S4 Table. Additional primary data, related to Figs 2 and 3.
(XLSX)

Acknowledgments

Author Contributions

Conceptualization: Flavia A. Graca, Natalie Sheffield, Melissa Puppa, Liam C. Hunt, Fabio Demontis.

Formal analysis: Flavia A. Graca, Natalie Sheffield, David Finkelstein, Fabio Demontis.

References

1. Bonaldo P, Sandri M. Cellular and molecular mechanisms of muscle atrophy. Disease models & mechanisms. 2013; 6(1):25–39. https://doi.org/10.1242/dmm.010389 PMID: 23268536; PubMed Central PMCID: PMC3529336.

2. Ciciliot S, Rossi AC, Dyar KA, Blaauw B, Schiaffino S. Muscle type and fiber type specificity in muscle wasting. The international journal of biochemistry & cell biology. 2013; 45(10):2191–9. https://doi.org/10.1016/j.biocel.2013.05.016 PMID: 23702032.

3. Cohen S, Nathan JA, Goldberg AL. Muscle wasting in disease: molecular mechanisms and promising therapies. Nat Rev Drug Discov. 2015; 14(1):58–74. Epub 2015/01/01. https://doi.org/10.1038/nrd4467 PMID: 25549588.

4. Zhou X, Wang JL, Lu J, Song Y, Kwak KS, Jiao Q, et al. Reversal of cancer cachexia and muscle wasting by ActRIIB antagonism leads to prolonged survival. Cell. 2010; 142(4):531–43. https://doi.org/10.1016/j.cell.2010.07.011 PMID: 20723755.

5. Tisdale MJ. Reversing cachexia. Cell. 2010; 142(4):511–2. https://doi.org/10.1016/j.cell.2010.08.004 PMID: 20723750.

6. Johnston AJ, Murphy KT, Jenkinson L, Laine D, Emmrich K, Faou P, et al. Targeting of Fn14 Prevents Cancer-Induced Cachexia and Prolongs Survival. Cell. 2015; 162(6):1365–78. https://doi.org/10.1016/j.cell.2015.08.031 PMID: 26359988.

7. Lecker SH, Jagoe RT, Gilbert A, Gomes M, Baracos V, Bailey J, et al. Multiple types of skeletal muscle atrophy involve a common program of changes in gene expression. FASEB journal: official publication of the Federation of American Societies for Experimental Biology. 2004; 18(1):39–51. https://doi.org/10.1096/fj.03-0610com PMID: 14718385.

8. Schiaffino S, Dyar KA, Ciciliot S, Blaauw B, Sandri M. Mechanisms regulating skeletal muscle growth and atrophy. FEBS J. 2013; 280(17):4294–314. https://doi.org/10.1111/febs.12253 PMID: 23517348.

9. Demontis F, Piccirillo R, Goldberg AL, Perrimon N. Mechanisms of skeletal muscle aging: insights from Drosophila and mammalian models. Dis Model Mech. 2013; 6(6):1339–52. https://doi.org/10.1242/dmm.012559 PMID: 24092876; PubMed Central PMCID: PMC3820258.

10. Piccirillo R, Demontis F, Perrimon N, Goldberg AL. Mechanisms of muscle growth and atrophy in mammals and Drosophila. Dev Dyn. 2014;(2) (243):201–15. https://doi.org/10.1002/dvdy.24036 PMID: 24038488.

11. Milan G, Romanello V, Pescatore F, Armani A, Paik JH, Frasson L, et al. Regulation of autophagy and the ubiquitin-proteasome system by the FoxO transcriptional network during muscle atrophy. Nat Commun. 2015; 6:6670. Epub 2015/04/11. https://doi.org/10.1038/ncomms7670 PMID: 25858807; PubMed Central PMCID: PMC4403316.

12. Judge SM, Wu CL, Beharry AW, Roberts BM, Ferreira LF, Kandarian SC, et al. Genome-wide identification of FoxO-dependent gene networks in skeletal muscle during C26 cancer cachexia. BMC Cancer. 2014; 14:997. https://doi.org/10.1186/1471-2407-14-997 PMID: 25539728; PubMed Central PMCID: PMC4391468.

13. Mammucari C, Milan G, Romanello V, Masiero E, Rudolf R, Del Piccolo P, et al. FoxO3 controls autophagy in skeletal muscle in vivo. Cell Metab. 2007; 6(6):458–71. https://doi.org/10.1016/j.cmet.2007.11.001 PMID: 18054315.

14. Schiaffino S, Mammucari C. Regulation of skeletal muscle growth by the IGF1-Akt/PKB pathway: insights from genetic models. Skeletal muscle. 2011; 1(1):4. https://doi.org/10.1186/2044-5040-1-4 PMID: 21798082; PubMed Central PMCID: PMC3143906.

15. Stitt TN, Drujan D, Clarke BA, Panaro F, Timofeyva Y, Kline WO, et al. The IGF-1/PI3K/Akt pathway prevents expression of muscle atrophy-induced ubiquitin ligases by inhibiting FOXO transcription factors. Mol Cell. 2004; 14(3):395–403. https://doi.org/10.1016/s1097-2765(04)00211-4 PMID: 15125842.

16. Zhao J, Brault JJ, Schild A, Cao P, Sandri M, Schiaffino S, et al. FoxO3 coordinately activates protein degradation by the autophagic/lysosomal and proteasomal pathways in atrophying muscle cells. Cell Metab. 2007; 6(6):472–83. Epub 2007/12/07. https://doi.org/10.1016/j.cmet.2007.11.004 PMID: 18054316.

17. Masiero E, Agatea L, Mammucari C, Blaauw B, Loro E, Komatsu M, et al. Autophagy is required to maintain muscle mass. Cell Metab. 2009; 10(6):507–15. https://doi.org/10.1016/j.cmet.2009.10.008 PMID: 19945408.

18. Vaquerizas JM, Kummerfeld SK, Teichmann SA, Luscombe NM. A census of human transcription factors: function, expression and evolution. Nat Rev Genet. 2009; 10(4):252–63. Epub 2009/03/11. https://doi.org/10.1038/nrg2538 PMID: 19274049.

19. Abmayr SM, Zhuang S, Geisbrecht ER. Myoblast fusion in Drosophila. Methods Mol Biol. 2008; 475:75–97. Epub 2008/11/04. https://doi.org/10.1007/978-1-59745-250-2_5 PMID: 18979239.

20. Bai J, Hartwig JH, Perrimon N. SALS, a WH2-domain-containing protein, promotes sarcomeric actin filament elongation from pointed ends during Drosophila muscle growth. Dev Cell. 2007; 13(6):828–42. https://doi.org/10.1016/j.devcel.2007.10.003 PMID: 18061565.

21. Balakrishnan M, Sisso WJ, Baylies MK. Analyzing muscle structure and function throughout the larval instars in live Drosophila. STAR Protoc. 2021; 2(1):100291. Epub 2021/02/04. https://doi.org/10.1016/j.xpro.2020.100291 PMID: 33532738; PubMed Central PMCID: PMC7821049.

22. Balakrishnan M, Yu SF, Chin SM, Soffar DB, Windner SE, Goode BL, et al. Cofilin Loss in Drosophila Muscles Contributes to Muscle Weakness through Defective Sarcomerogenesis during Muscle Growth. Cell Rep. 2020; 32(3):107893. Epub 2020/07/23. https://doi.org/10.1016/j.celrep.2020.107893 PMID: 32697999; PubMed Central PMCID: PMC7479987.

23. Bawa S, Gameros S, Baumann K, Brooks DS, Kollhoff JA, Zolkiewski M, et al. Costameric integrin and sarcoglycan protein levels are altered in a Drosophila model for Limb-girdle muscular dystrophy type 2H. Mol Biol Cell. 2021; 32(3):260–73. Epub 2020/12/10. https://doi.org/10.1091/mbc.E20-07-0453 PMID: 33296226; PubMed Central PMCID: PMC8098830.

24. Bawa S, Piccirillo R, Geisbrecht ER. TRIM32: A Multifunctional Protein Involved in Muscle Homeostasis, Glucose Metabolism, and Tumorigenesis. Biomolecules. 2021; 11(3). Epub 2021/04/04. https://doi.org/10.3390/biom11030408 PMID: 33802079; PubMed Central PMCID: PMC7999776.

25. Bothe I, Baylies MK. Drosophila myogenesis. Curr Biol. 2016; 26(17):R786–91. Epub 2016/09/14. https://doi.org/10.1016/j.cub.2016.07.062 PMID: 27623256; PubMed Central PMCID: PMC5204462.

26. Brooks D, Naeem F, Stetsiv M, Goetting SC, Bawa S, Green N, et al. Drosophila NUAK functions with Starvin/BAG3 in autophagic protein turnover. PLoS Genet. 2020; 16(4):e1008700. Epub 2020/04/23. https://doi.org/10.1371/journal.pgen.1008700 PMID: 32320396; PubMed Central PMCID: PMC7176095.

27. Dobi KC, Schulman VK, Baylies MK. Specification of the somatic musculature in Drosophila. Wiley Interdiscip Rev Dev Biol. 2015; 4(4):357–75. Epub 2015/03/03. https://doi.org/10.1002/wdev.182 PMID: 25728002; PubMed Central PMCID: PMC4456285.

28. Green N, Walker J, Bontrager A, Zych M, Geisbrecht ER. A tissue communication network coordinating innate immune response during muscle stress. J Cell Sci. 2018; 131(24). Epub 2018/11/28. https://doi.org/10.1242/jcs.217943 PMID: 30478194; PubMed Central PMCID: PMC6307882.

29. Kim MJ, O'Connor MB. Drosophila Activin signaling promotes muscle growth through InR/TORC1-dependent and -independent processes. Development. 2021; 148(1). Epub 2020/11/26. https://doi.org/10.1242/dev.190868 PMID: 33234715; PubMed Central PMCID: PMC7823159.

30. LaBeau-DiMenna EM, Clark KA, Bauman KD, Parker DS, Cripps RM, Geisbrecht ER. Thin, a Trim32 ortholog, is essential for myofibril stability and is required for the integrity of the costamere in Drosophila. Proc Natl Acad Sci U S A. 2012; 109(44):17983–8. Epub 2012/10/17. https://doi.org/10.1073/pnas.1208408109 PMID: 23071324; PubMed Central PMCID: PMC3497806.

31. Morriss GR, Bryantsev AL, Chechenova M, LaBeau EM, Lovato TL, Ryan KM, et al. Analysis of skeletal muscle development in Drosophila. Methods Mol Biol. 2012; 798:127–52. https://doi.org/10.1007/978-1-61779-343-1_8 PMID: 22130835.

32. Rui Y, Bai J, Perrimon N. Sarcomere formation occurs by the assembly of multiple latent protein complexes. PLoS Genet. 2010; 6(11):e1001208. Epub 2010/12/03. https://doi.org/10.1371/journal.pgen.1001208 PMID: 21124995; PubMed Central PMCID: PMC2987826.

33. Schejter ED, Baylies MK. Born to run: creating the muscle fiber. Curr Opin Cell Biol. 2010; 22(5):566–74. Epub 2010/09/08. https://doi.org/10.1016/j.ceb.2010.08.009 PMID: 20817426; PubMed Central PMCID: PMC3903116.

34. Schulman VK, Dobi KC, Baylies MK. Morphogenesis of the somatic musculature in Drosophila melanogaster. Wiley Interdiscip Rev Dev Biol. 2015; 4(4):313–34. Epub 2015/03/12. https://doi.org/10.1002/wdev.180 PMID: 25758712; PubMed Central PMCID: PMC4456235.

35. Demontis F, Perrimon N. Integration of Insulin receptor/Foxo signaling and dMyc activity during muscle growth regulates body size in Drosophila. Development. 2009; 136(6):983–93. https://doi.org/10.1242/dev.027466 PMID: 19211682.

36. Hunt LC, Schadeberg B, Stover J, Haugen B, Pagala V, Wang YD, et al. Antagonistic control of myofiber size and muscle protein quality control by the ubiquitin ligase UBR4 during aging. Nat Commun. 2021; 12(1):1418. Epub 2021/03/05. https://doi.org/10.1038/s41467-021-21738-8 PMID: 33658508.

37. Hunt LC, Stover J, Haugen B, Shaw TI, Li Y, Pagala VR, et al. A Key Role for the Ubiquitin Ligase UBR4 in Myofiber Hypertrophy in Drosophila and Mice. Cell reports. 2019; 28(5):1268–81 e6. https://doi.org/10.1016/j.celrep.2019.06.094 PMID: 31365869; PubMed Central PMCID: PMC6697171.

38. Rhee DY, Cho DY, Zhai B, Slattery M, Ma L, Mintseris J, et al. Transcription factor networks in Drosophila melanogaster. Cell Rep. 2014; 8(6):2031–43. Epub 2014/09/23. https://doi.org/10.1016/j.celrep.2014.08.038 PMID: 25242320; PubMed Central PMCID: PMC4403667.

39. Pilot-Storck F, Chopin E, Rual JF, Baudot A, Dobrokhotov P, Robinson-Rechavi M, et al. Interactome mapping of the phosphatidylinositol 3-kinase-mammalian target of rapamycin pathway identifies deformed epidermal autoregulatory factor-1 as a new glycogen synthase kinase-3 interactor. Molecular & cellular proteomics: MCP. 2010; 9(7):1578–93. Epub 2010/04/07. https://doi.org/10.1074/mcp.M900568-MCP200 PMID: 20368287; PubMed Central PMCID: PMC2938100.

40. Verhees KJ, Schols AM, Kelders MC, Op den Kamp CM, van der Velden JL, Langen RC. Glycogen synthase kinase-3beta is required for the induction of skeletal muscle atrophy. Am J Physiol Cell Physiol. 2011; 301(5):C995–C1007. Epub 2011/08/13. https://doi.org/10.1152/ajpcell.00520.2010 PMID: 21832246.

41. Aweida D, Rudesky I, Volodin A, Shimko E, Cohen S. GSK3-beta promotes calpain-1-mediated desmin filament depolymerization and myofibril loss in atrophy. The Journal of cell biology. 2018; 217(10):3698–714. Epub 2018/08/01. https://doi.org/10.1083/jcb.201802018 PMID: 30061109; PubMed Central PMCID: PMC6168250.

42. Lecker SH, Solomon V, Price SR, Kwon YT, Mitch WE, Goldberg AL. Ubiquitin conjugation by the N-end rule pathway and mRNAs for its components increase in muscles of diabetic rats. The Journal of clinical investigation. 1999; 104(10):1411–20. https://doi.org/10.1172/JCI7300 PMID: 10562303; PubMed Central PMCID: PMC409840.

43. Solomon V, Lecker SH, Goldberg AL. The N-end rule pathway catalyzes a major fraction of the protein degradation in skeletal muscle. The Journal of biological chemistry. 1998; 273(39):25216–22. https://doi.org/10.1074/jbc.273.39.25216 PMID: 9737984.

44. Ranganayakulu G, Zhao B, Dokidis A, Molkentin JD, Olson EN, Schulz RA. A series of mutations in the D-MEF2 transcription factor reveal multiple functions in larval and adult myogenesis in Drosophila. Developmental biology. 1995; 171(1):169–81. https://doi.org/10.1006/dbio.1995.1269 PMID: 7556894.

45. Park J, Lee SB, Lee S, Kim Y, Song S, Kim S, et al. Mitochondrial dysfunction in Drosophila PINK1 mutants is complemented by parkin. Nature. 2006; 441(7097):1157–61. https://doi.org/10.1038/nature04788 PMID: 16672980.

46. Klein P, Muller-Rischart AK, Motori E, Schonbauer C, Schnorrer F, Winklhofer KF, et al. Ret rescues mitochondrial morphology and muscle degeneration of Drosophila Pink1 mutants. EMBO J. 2014; 33(4):341–55. Epub 2014/01/30. https://doi.org/10.1002/embj.201284290 PMID: 24473149; PubMed Central PMCID: PMC3983680.

47. Boutet SC, Biressi S, Iori K, Natu V, Rando TA. Taf1 regulates Pax3 protein by monoubiquitination in skeletal muscle progenitors. Mol Cell. 2010; 40(5):749–61. Epub 2010/12/15. https://doi.org/10.1016/j.molcel.2010.09.029 PMID: 21145483; PubMed Central PMCID: PMC3023311.

48. Mal AK. Histone methyltransferase Suv39h1 represses MyoD-stimulated myogenic differentiation. EMBO J. 2006; 25(14):3323–34. Epub 2006/07/22. https://doi.org/10.1038/sj.emboj.7601229 PMID: 16858404; PubMed Central PMCID: PMC1523181.

49. Kuttenkeuler D, Pelte N, Ragab A, Gesellchen V, Schneider L, Blass C, et al. A large-scale RNAi screen identifies Deaf1 as a regulator of innate immune responses in Drosophila. J Innate Immun. 2010; 2(2):181–94. Epub 2010/04/09. https://doi.org/10.1159/000248649 PMID: 20375635.

50. Veraksa A, Kennison J, McGinnis W. DEAF-1 function is essential for the early embryonic development of Drosophila. Genesis. 2002; 33(2):67–76. Epub 2002/07/12. https://doi.org/10.1002/gene.10090 PMID: 12112874.

51. Gross CT, McGinnis W. DEAF-1, a novel protein that binds an essential region in a Deformed response element. EMBO J. 1996; 15(8):1961–70. Epub 1996/04/15. PMID: 8617243; PubMed Central PMCID: PMC450115.

52. Reed DE, Huang XM, Wohlschlegel JA, Levine MS, Senger K. DEAF-1 regulates immunity gene expression in Drosophila. Proc Natl Acad Sci U S A. 2008; 105(24):8351–6. Epub 2008/06/14. https://doi.org/10.1073/pnas.0802921105 PMID: 18550807; PubMed Central PMCID: PMC2448840.

53. Rajab A, Schuelke M, Gill E, Zwirner A, Seifert F, Morales Gonzalez S, et al. Recessive DEAF1 mutation associates with autism, intellectual disability, basal ganglia dysfunction and epilepsy. J Med Genet. 2015; 52(9):607–11. Epub 2015/06/07. https://doi.org/10.1136/jmedgenet-2015-103083 PMID: 26048982.

54. Gund C, Powis Z, Alcaraz W, Desai S, Baranano K. Identification of a syndrome comprising microcephaly and intellectual disability but not white matter disease associated with a homozygous c.676C>T p. R226W DEAF1 mutation. Am J Med Genet A. 2016; 170A(5):1330–2. Epub 2016/02/03. https://doi.org/10.1002/ajmg.a.37580 PMID: 26834045.

55. Sumathipala DS, Misceo D, Larsen SM, Baroy T, Gamage TH, Frengen E, et al. A girl with a neurodevelopmental syndrome, adducted thumbs and frequent infections caused by novel homozygous variant in DEAF1. Clin Dysmorphol. 2020; 29(2):107–10. Epub 2020/01/14. https://doi.org/10.1097/MCD.0000000000000314 PMID: 31929336.

56. Rommel C, Bodine SC, Clarke BA, Rossman R, Nunez L, Stitt TN, et al. Mediation of IGF-1-induced skeletal myotube hypertrophy by PI(3)K/Akt/mTOR and PI(3)K/Akt/GSK3 pathways. Nature cell biology. 2001; 3(11):1009–13. https://doi.org/10.1038/ncb1101-1009 PMID: 11715022.

57. Bawa S, Brooks DS, Neville KE, Tipping M, Sagar MA, Kollhoff JA, et al. Drosophila TRIM32 cooperates with glycolytic enzymes to promote cell growth. Elife. 2020; 9. Epub 2020/04/01. https://doi.org/10.7554/eLife.52358 PMID: 32223900; PubMed Central PMCID: PMC7105379.

58. Tixier V, Bataille L, Etard C, Jagla T, Weger M, Daponte JP, et al. Glycolysis supports embryonic muscle growth by promoting myoblast fusion. Proc Natl Acad Sci U S A. 2013; 110(47):18982–7. Epub 2013/11/06. https://doi.org/10.1073/pnas.1301262110 PMID: 24191061; PubMed Central PMCID: PMC3839714.

59. Ugur B, Chen K, Bellen HJ. Drosophila tools and assays for the study of human diseases. Dis Model Mech. 2016; 9(3):235–44. Epub 2016/03/05. https://doi.org/10.1242/dmm.023762 PMID: 26935102; PubMed Central PMCID: PMC4833332.

60. Badenhorst P, Xiao H, Cherbas L, Kwon SY, Voas M, Rebay I, et al. The Drosophila nucleosome remodeling factor NURF is required for Ecdysteroid signaling and metamorphosis. Genes Dev. 2005; 19(21):2540–5. Epub 2005/11/03. https://doi.org/10.1101/gad.1342605 PMID: 16264191; PubMed Central PMCID: PMC1276728.

61. Aoyagi N, Wassarman DA. Genes encoding Drosophila melanogaster RNA polymerase II general transcription factors: diversity in TFIIA and TFIID components contributes to gene-specific transcriptional regulation. J Cell Biol. 2000; 150(2):F45–50. Epub 2000/07/26. https://doi.org/10.1083/jcb.150.2.f45 PMID: 10908585; PubMed Central PMCID: PMC2180226.

62. Fan W, Lam SM, Xin J, Yang X, Liu Z, Liu Y, et al. Drosophila TRF2 and TAF9 regulate lipid droplet size and phospholipid fatty acid composition. PLoS Genet. 2017; 13(3):e1006664. Epub 2017/03/09. https://doi.org/10.1371/journal.pgen.1006664 PMID: 28273089; PubMed Central PMCID: PMC5362240.

63. Fukawa T, Yan-Jiang BC, Min-Wen JC, Jun-Hao ET, Huang D, Qian CN, et al. Excessive fatty acid oxidation induces muscle atrophy in cancer cachexia. Nat Med. 2016; 22(6):666–71. Epub 2016/05/03. https://doi.org/10.1038/nm.4093 PMID: 27135739.

64. Heigwer F, Port F, Boutros M. RNA Interference (RNAi) Screening in Drosophila. Genetics. 2018; 208(3):853–74. Epub 2018/03/01. https://doi.org/10.1534/genetics.117.300077 PMID: 29487145; PubMed Central PMCID: PMC5844339.

65. Hayashi S, Kondo T. Development and Function of the Drosophila Tracheal System. Genetics. 2018; 209(2):367–80. https://doi.org/10.1534/genetics.117.300167 PMID: 29844090; PubMed Central PMCID: PMC5972413.

66. Sopko R, Foos M, Vinayagam A, Zhai B, Binari R, Hu Y, et al. Combining genetic perturbations and proteomics to examine kinase-phosphatase networks in Drosophila embryos. Dev Cell. 2014; 31(1):114–27. Epub 2014/10/07. https://doi.org/10.1016/j.devcel.2014.07.027 PMID: 25284370; PubMed Central PMCID: PMC4208667.

67. Crittenden JR, Skoulakis EMC, Goldstein ES, Davis RL. Drosophila mef2 is essential for normal mushroom body and wing development. Biol Open. 2018; 7(9). Epub 2018/08/18. https://doi.org/10.1242/bio.035618 PMID: 30115617; PubMed Central PMCID: PMC6176937.

68. Zhu J, Thompson CB. Metabolic regulation of cell growth and proliferation. Nature reviews Molecular cell biology. 2019; 20(7):436–50. Epub 2019/04/13. https://doi.org/10.1038/s41580-019-0123-5 PMID: 30976106; PubMed Central PMCID: PMC6592760.

69. Pansters NA, Schols AM, Verhees KJ, de Theije CC, Snepvangers FJ, Kelders MC, et al. Muscle-specific GSK-3beta ablation accelerates regeneration of disuse-atrophied skeletal muscle. Biochim Biophys Acta. 2015; 1852(3):490–506. Epub 2014/12/17. https://doi.org/10.1016/j.bbadis.2014.12.006 PMID: 25496993.

70. Verhees KJ, Pansters NA, Baarsma HA, Remels AH, Haegens A, de Theije CC, et al. Pharmacological inhibition of GSK-3 in a guinea pig model of LPS-induced pulmonary inflammation: II. Effects on skeletal muscle atrophy. Respir Res. 2013; 14:117. Epub 2013/11/05. https://doi.org/10.1186/1465-9921-14-117 PMID: 24180420; PubMed Central PMCID: PMC4176095.

71. Verhees KJ, Pansters NA, Schols AM, Langen RC. Regulation of skeletal muscle plasticity by glycogen synthase kinase-3beta: a potential target for the treatment of muscle wasting. Curr Pharm Des. 2013; 19(18):3276–98. Epub 2012/11/16. https://doi.org/10.2174/1381612811319180011 PMID: 23151136.

72. Graham JR, Tullai JW, Cooper GM. GSK-3 represses growth factor-inducible genes by inhibiting NF-kappaB in quiescent cells. J Biol Chem. 2010; 285(7):4472–80. Epub 2009/12/19. https://doi.org/10.1074/jbc.M109.053785 PMID: 20018891; PubMed Central PMCID: PMC2836053.

73. Hayes JD, Chowdhry S, Dinkova-Kostova AT, Sutherland C. Dual regulation of transcription factor Nrf2 by Keap1 and by the combined actions of beta-TrCP and GSK-3. Biochem Soc Trans. 2015; 43 (4):611–20. Epub 2015/11/10. https://doi.org/10.1042/BST20150011 PMID: 26551701.

74. Ngeow KC, Friedrichsen HJ, Li L, Zeng Z, Andrews S, Volpon L, et al. BRAF/MAPK and GSK3 signaling converges to control MITF nuclear export. Proc Natl Acad Sci U S A. 2018; 115(37):E8668–E77. Epub 2018/08/29. https://doi.org/10.1073/pnas.1810498115 PMID: 30150413; PubMed Central PMCID: PMC6140509.

75. Sutherland C. What Are the bona fide GSK3 Substrates? Int J Alzheimers Dis. 2011; 2011:505607. Epub 2011/06/02. https://doi.org/10.4061/2011/505607 PMID: 21629754; PubMed Central PMCID: PMC3100594.

76. Tullai JW, Chen J, Schaffer ME, Kamenetsky E, Kasif S, Cooper GM. Glycogen synthase kinase-3 represses cyclic AMP response element-binding protein (CREB)-targeted immediate early genes in quiescent cells. J Biol Chem. 2007; 282(13):9482–91. Epub 2007/02/06. https://doi.org/10.1074/jbc.M700067200 PMID: 17277356; PubMed Central PMCID: PMC1839957.

77. Tullai JW, Graham JR, Cooper GM. A GSK-3-mediated transcriptional network maintains repression of immediate early genes in quiescent cells. Cell Cycle. 2011; 10(18):3072–7. Epub 2011/09/09. https://doi.org/10.4161/cc.10.18.17321 PMID: 21900749; PubMed Central PMCID: PMC3218618.

78. Hu Y, Flockhart I, Vinayagam A, Bergwitz C, Berger B, Perrimon N, et al. An integrative approach to ortholog prediction for disease-focused and other functional studies. BMC Bioinformatics. 2011; 12:357. https://doi.org/10.1186/1471-2105-12-357 PMID: 21880147; PubMed Central PMCID: PMC3179972.

79. Demontis F, Perrimon N. FOXO/4E-BP signaling in Drosophila muscles regulates organism-wide proteostasis during aging. Cell. 2010; 143(5):813–25. https://doi.org/10.1016/j.cell.2010.10.007 PMID: 21111239; PubMed Central PMCID: PMC3066043.

80. Bourouis M. Targeted increase in shaggy activity levels blocks wingless signaling. Genesis. 2002; 34 (1–2):99–102. Epub 2002/09/27. https://doi.org/10.1002/gene.10114 PMID: 12324959.

81. Hunt LC, Jiao J, Wang YD, Finkelstein D, Rao D, Curley M, et al. Circadian gene variants and the skeletal muscle circadian clock contribute to the evolutionary divergence in longevity across Drosophila populations. Genome Res. 2019; 29(8):1262–76. https://doi.org/10.1101/gr.246884.118 PMID: 31249065; PubMed Central PMCID: PMC6673717.

82. Hunt LC, Xu B, Finkelstein D, Fan Y, Carroll PA, Cheng PF, et al. The glucose-sensing transcription factor MLX promotes myogenesis via myokine signaling. Genes Dev. 2015; 29(23):2475–89. https://doi.org/10.1101/gad.267419.115 PMID: 26584623; PubMed Central PMCID: PMC4691951.

83. Dobin A, Davis CA, Schlesinger F, Drenkow J, Zaleski C, Jha S, et al. STAR: ultrafast universal RNA-seq aligner. Bioinformatics. 2013; 29(1):15–21. https://doi.org/10.1093/bioinformatics/bts635 PMID: 23104886; PubMed Central PMCID: PMC3530905.

84. Anders S, Pyl PT, Huber W. HTSeq—a Python framework to work with high-throughput sequencing data. Bioinformatics. 2015; 31(2):166–9. https://doi.org/10.1093/bioinformatics/btu638 PMID: 25260700; PubMed Central PMCID: PMC4287950.

85. Robinson MD, McCarthy DJ, Smyth GK. edgeR: a Bioconductor package for differential expression analysis of digital gene expression data. Bioinformatics. 2010; 26(1):139–40. https://doi.org/10.1093/bioinformatics/btp616 PMID: 19910308; PubMed Central PMCID: PMC2796818.

86. Law CW, Chen Y, Shi W, Smyth GK. voom: Precision weights unlock linear model analysis tools for RNA-seq read counts. Genome Biol. 2014; 15(2):R29. https://doi.org/10.1186/gb-2014-15-2-r29 PMID: 24485249; PubMed Central PMCID: PMC4053721.

87. Ritchie ME, Phipson B, Wu D, Hu Y, Law CW, Shi W, et al. limma powers differential expression analyses for RNA-sequencing and microarray studies. Nucleic Acids Res. 2015; 43(7):e47. https://doi.org/10.1093/nar/gkv007 PMID: 25605792; PubMed Central PMCID: PMC4402510.

88. Huang da W, Sherman BT, Lempicki RA. Systematic and integrative analysis of large gene lists using DAVID bioinformatics resources. Nat Protoc. 2009; 4(1):44–57. https://doi.org/10.1038/nprot.2008.211 PMID: 19131956.